Isolation and Characterization of Glutaminyl Cyclases from *Drosophila*: Evidence for Enzyme Forms with Different Subcellular Localization

Stephan Schilling,[‡] Christiane Lindner,[§] Birgit Koch,[‡] Michael Wermann,[‡] Jens-Ulrich Rahfeld,[‡] Alex von Bohlen,[||] Thomas Rudolph,[§] Gunter Reuter,[§] and Hans-Ulrich Demuth*,[‡]

Probiodrug AG, Weinbergweg 22, 06120 Halle/Saale, Germany, Institute of Genetics, Martin-Luther-University, Weinbergweg 19, 06120 Halle/Saale, Germany, and Institute for Analytical Sciences, Bunsen-Kirchhoff-Strasse 11, D-44139 Dortmund, Germany

Received May 29, 2007; Revised Manuscript Received July 14, 2007

ABSTRACT: Glutaminyl cyclases (QCs) present in plants and vertebrates catalyze the formation of pyroglutamic acid (pGlu) from N-terminal glutamine. Pyroglutamyl hormones also identified in invertebrates imply the involvement of QC activity during their posttranslational maturation. Database mining led to the identification of two genes in *Drosophila*, which putatively encode QCs, CG32412 (DromeQC) and CG5976 (isoDromeQC). Analysis of their primary structure suggests different subcellular localizations. While DromeQC appeared to be secreted due to an N-terminal signal peptide, isoDromeQC contains either an N-terminal mitochondrial targeting or a secretion signal due to generation of different transcripts from gene CG5976. According to the prediction, homologous expression of the corresponding cDNAs in S2 cells revealed either secreted protein in the medium or intracellular QC activity. Subcellular fractionation and immunochemistry support export of isoDromeQC into the mitochondrion. For enzymatic characterization, DromeQC and isoDromeQC were expressed heterologously in *Pichia pastoris* and *Escherichia coli*, respectively. Compared to mammalian QCs, the specificity constants were about 1 order of magnitude lower for most of the analyzed substrates. The pH dependence of the specificity constant was similar for both enzymes, indicating the necessity of an unprotonated substrate amino group and two protonated groups of the enzyme, resulting in an asymmetric bell-shaped characteristic. The determination of the metal content of DromeQC revealed equimolar protein-bound zinc. These results prove conserved enzymatic mechanisms between QCs from invertebrates and mammals. *Drosophila* is the first organism for which isoenzymes of glutaminyl cyclase have been isolated. The identification of a mitochondrial QC points toward yet undiscovered physiological functions of these enzymes.

Pyroglutamic acid (pGlu)[1] is generated from N-terminal glutamine during prohormone maturation in the secretory pathway (*1*, *2*). Also, the conversion of N-terminal glutamic acid into pGlu has been described in vivo, which possibly has implications in the development of amyloidotic diseases (*3*−*5*). Glutaminyl cyclases (QCs) have been identified to catalyze the cyclization of N-terminal glutaminyl and glutamyl residues in plants and vertebrates (*6*−*8*). Although the results of several studies support similar catalytic properties of the enzymes from these origins, structural investigations clearly reveal different evolutionary origins of plant and animal QCs (*9*−*11*). Apparently, the proteins developed due to convergent evolution, since most recent results suggest similar physiological functions.

First tissue distribution studies of mammalian QCs resulted that they are mainly expressed in brain and some peripheral glands, e.g., thyroid and thymus (*12*−*14*). It is expected that the enzyme is directed to the regulated secretory pathway of the expressing cells where the hormone maturation process takes place (*14*). Upon stimulation, QCs appear to be secreted from the cells together with the mature hormones.

Pyroglutamyl peptides and proteins were also identified in invertebrates, suggesting that this peptide modification represents an evolutionarily conserved modification, mediating receptor interaction or protein stabilization. For instance, the adipokinetic hormone and corazonin, neuropeptides regulating the glucose concentration in the hemolymph and the heart beat in arthropods, respectively, have been identified as pGlu peptides (*15*, *16*).

These findings tempted us to isolate and characterize a QC from an invertebrate origin, the fruit fly *Drosophila melanogaster*, which acts as a well-characterized model organism, preferably in genetic analyses. Interestingly, the homology search led to identification of two chromosomal regions, which encode glutaminyl cyclases with different subcellular localizations, suggesting different, yet undiscovered physiological functions of the gene products.

EXPERIMENTAL PROCEDURES

Materials. Chemicals were purchased as follows: glutamate dehydrogenase from Fluka, pyroglutamyl aminopeptidase from Qiagen, H-Gln-AMC, H-Gln-βNA, and the glutaminyl

* To whom correspondence should be addressed. Phone: 49 345 5559900. Fax: 49 345 5559901. E-mail: Hans-Ulrich.Demuth@probiodrug.de.

[‡] Probiodrug AG.

[§] Martin-Luther-University.

[||] Institute for Analytical Sciences.

[1] Abbreviations: QC, glutaminyl cyclase; pGlu, pyroglutamic acid.

10.1021/bi701043x CCC: $37.00
Published on Web 08/28/2007

Table 1: Oligonucleotides Applied for Cloning and Expression of DomeQC and isoDromeQC

primer	sequence (5′ → 3′)	restriction site for cloning	expression
A	TATATA*GAATTC*TGCGTCGCCGAGCTCTGAAGC	*Eco*RI	S2 cells
A	TATATA*ACCGGT*CTATGTTCGGTAAAAACGCAAATT	*Age*I	S2 cells
B	TATATA*GAATTC*TGCGTCGCCGAGCTCTGAAGC	*Eco*RI	S2 cells
B	TATATA*ACCGGT*TGTTCGGTAAAAACGCAAATT	*Age*I	S2 cells
C	TATATA*GAATTC*GGTGTGTTGTGTAGTGTTCTG	*Eco*RI	S2 cells
C	TATATA*ACCGGT*CTACTTGGCCTCGGTTCCGGCCAG	*Age*I	S2 cells
D	TATATA*GAATTC*GGTGTGTTGTGTAGTGTTCTG	*Eco*RI	S2 cells
D	TATATA*ACCGGT*CTTGGCCTCGGTTCCGGCCAG	*Age*I	S2 cells
E	ATATAT*CTCGAG*AAAAGAAACATTGGATCCCAGTGGCGC	*Xho*I	*P. pastoris*
E	ATATAT*GCGGCCGC*CTATGTTCGGTAAAAACGCAAATT	*Not*I	*P. pastoris*
F	AATATA*GGATCCA*TTCGAACTGGTGGATATTCC	*Bam*HI	*E. coli*
F	ATATA*GCATGCC*TACTTGGCCTCGGTTCCGGCC	*Sph*I	*E. coli*

dipeptides from Bachem, NADH/H^+ and α-ketoglutaric acid from Sigma, and the imidazole derivatives from Acros and Aldrich. The glutaminyl tri- and tetrapeptides were synthesized as described previously (*17*). All other chemicals were of analytical or HPLC grade.

Cloning Procedures and Expression. The primers for isolation of the open reading frame of DromeQC and isoDromeQC were designed using the coding sequences of the genes CG32412 and CG5976, respectively [http://flybase.bio.indiana.edu/ (*18*)]. The open reading frames of CG32412, CG5976A, and CG5976B were isolated from EST clones GH11174 (adult head), RE53796 (embryo), and RE61650 (embryo), respectively. For expression studies of both cDNAs, the coding sequences were amplified by PCR using the primers listed in Table 1. Expression of DromeQC and isoDromeQC in S2 *Drosophila* cells was carried out either as the native protein or as C-terminally poly-His-tagged proteins. The cDNA fragments were amplified using the primer pairs A−D. The digested fragments were ligated into the vector pMTV5HisB (Invitrogen), propagated in *Escherichia coli*, and verified by sequencing of the sense and antisense strand. S2 cells were stably transfected according to the manufacturer's instructions (Invitrogen). Selection was done in blasticidin-containing medium (20 μg/mL). Protein expression was induced by 500 μM $Cu^{II}SO_4$. Cells were harvested after 24−48 h of expression.

For enzymological studies, DromeQC and isoDromeQC were heterologously expressed in *Pichia pastoris* and *E. coli*, respectively. The coding sequence of mature DromeQC was amplified using primer pair E (Table 1). The digested fragment was ligated into pPICZαB (Invitrogen) and propagated in *E. coli* JM109, and the sequence was verified. Plasmid DNA (1−2 μg) was applied for transformation of competent *P. pastoris* cells by electroporation according to the manufacturer's instructions (Bio-Rad). Selection was performed on plates containing 100 μg/mL zeocin. In order to test the recombinant yeast clones upon DromeQC expression, recombinants were grown at 30 °C for 24 h in 10 mL conical tubes containing 2 mL of BMGY. Afterward, the yeast was centrifuged and resuspended in 2 mL of BMMY containing 0.5% methanol. This concentration was maintained by addition of methanol every 24 h for about 72 h. Subsequently, QC activity in the supernatant was determined. Clones that displayed the highest activity were chosen for further experiments and fermentation.

For expression of isoDromeQC, primer pair F (Table 1) was used for amplification of the coding sequence of the mature protein, and the digested DNA fragment was ligated into pQE31 (Qiagen, Hilden, Germany). The plasmid was transformed into M15 cells (Qiagen) and grown on selective LB agar plates at 37 °C. Protein expression was studied in LB medium at room temperature. When the culture reached an OD_{600} of approximately 0.8, expression was induced with 0.2 mM IPTG overnight. Afterward, cells were collected, resuspended in 50 mM phosphate, pH 7.5, containing 1 mg/mL lysozome, and subjected to 10 cycles of sonification, followed by determination of QC activity.

Immunohistochemical Staining of S2 Cells. S2 cells were immunostained essentially as described (*19*). Post induction (24−48 h), 250 nM Mitotracker was applied to the cell culture before transfer to Lab Tek II chamber slides (Nunc) and allowed to settle down for 20 min. Medium and remaining cells were removed, and chambers were washed with PBS (3 × 10 min). Cells were fixed with ice-cold methanol for 20 min and washed with PBTA for 20 min. Primary antibody (mouse anti V5, 1:200 diluted in PBTA) was applied overnight at 4 °C with moderate shaking. Cells were washed with PBTA (3 × 10 min). Secondary antibody [goat anti-rabbit conjugated with Alexa488 (Molecular Probes), 1:200 diluted in PBTA] was applied for 2 h at room temperature with moderate shaking. Cells were washed with PBTA (3 × 10 min) and counterstained with DAPI (0.2 μg/mL) for 3 min. After PBTA washing, cells were mounted with Citifluor (Agar-Scientific). Staining was analyzed using a confocal laser-scanning microscope equipped with LSM510 software (Carl Zeiss).

Large-Scale Expression and Purification. The expression of DromeQC was performed in a 5.0 L bioreactor (Biostad B; B. Braun Biotech, Melsungen, Germany), essentially as described for expression of human QC in *P. pastoris* (*20*). Briefly, fermentation was carried out in basal salt medium supplemented with trace salts at pH 5.5. Biomass was accumulated in a glycerol batch and fed batch phase for about 28 h. Expression of QC was initiated by methanol feeding for an entire fermentation time of 72−78 h. After the cells were collected by centrifugation steps at 6000*g*, turbidity was removed from the DromeQC-containing supernatant by an additional centrifugation at 38000*g* for 4 h. For purification, the fermentation broth was diluted with water to a conductivity of about 5 mS/cm and applied in reversed-flow direction (15 mL/min) onto a Streamline SP XL column (2.5 × 100 cm) equilibrated with 0.05 M phosphate buffer, pH 6.0. Proteins were eluted at a flow rate of 8 mL/min using 0.15 M Tris-HCl buffer, pH 7.6, containing 1.5 M NaCl in

forward direction. QC-containing fractions were pooled, and ammonium sulfate was added to a final concentration of 1.2 M. The resulting solution was applied onto a butyl-Sepharose FF column (1.6 × 13 cm) at a flow rate of 4 mL/min. Afterward, 0.05 M phosphate buffer, pH 6.8, containing 0.75 M ammonium sulfate was applied for 5 column volumes. Homogeneous QC was eluted in reversed-flow direction using 0.05 M phosphate buffer, pH 6.8. The fractions containing DromeQC were pooled, concentrated, and applied onto a Sephadex G-25 fast desalting column (1.0 × 10 cm), which was preequilibrated in 50 mM Tris-HCl, pH 7.5, containing 100 mM NaCl. The purified DromeQC was stored at 4 °C for up to 2 weeks. For long-term storage, protein was shock-frozen in liquid nitrogen and stored at −80 °C.

IsoDromeQC was expressed in shake-flask cultures. Bacteria were collected by centrifugation at 6000*g*, resuspended in 50 mM phosphate buffer, pH 7.5, containing 1.0 mg/mL lysozome, and frozen. The thawed suspension was subjected to one cycle of high-pressure homogenization. Subsequently, the cleared supernatant (35000*g*, 2 h) was diluted to a final protein concentration of 1.0 mg/mL using phosphate-buffered saline containing 0.5 mM histidine and applied in reversed-flow direction (19 mL/min) onto a Streamline chelating column (2.5 × 100 cm) equilibrated with PBS. Proteins were eluted at a flow rate of 8.0 mL/min using 50 mM phosphate buffer, pH 6.8, containing 100 mM histidine. IsoDromeQC-containing fractions were pooled, and ammonium sulfate was added to a final concentration of 1.0 M. The resulting solution was applied onto a butyl-Sepharose FF column (1.6 × 13 cm) at a flow rate of 4 mL/min. Bound isoDromeQC was washed by applying 50 mM phosphate buffer, pH 6.8, and 0.8 M ammonium sulfate and eluted with 50 mM phosphate buffer, pH 6.8. Fractions containing QC activity were pooled and desalted. The purified isoDromeQC was stored at 4 °C for up to 2 weeks. For long-term storage, protein was shock-frozen in liquid nitrogen and stored at −80 °C.

Subcellular Fractionation. Subcellular fractionation of *Drosophila* S2 cells was performed essentially as described (*19*). Briefly, lysates of 5×10^7−1×10^6 cells were prepared using a Dounce homogenizer using a buffer consisting of 50 mM Pipes, pH 7.9, 50 mM KCl, 2.0 mM $MgCl_2$, 1.0 mM DTT, and 1.0 mM PMSF. The cellular fractions were prepared by sequential centrifugation steps at 700*g*, 24000*g*, and 54000*g*, resulting in a cell debris/nuclei pellet, a heavy membrane fraction, which is enriched for mitochondria, a light membrane fraction containing ER and plasma membrane, and the supernatant containing cytosolic proteins. Pellets were resuspended in 50 mM Tris-HCl, pH 7.5, containing 0.5% Triton X-100, and the QC activity was determined (pH 8.0) using H-Gln-βNA as a QC substrate.

QC Assays. QC activity was assayed fluorometrically or spectrophotometrically essentially as described (*21*−*23*). The assay reactions (250 μL) consisted of varying concentrations of H-Gln-AMC, H-Gln-βNA, or another glutaminyl peptide in 0.05 M Tris-HCl, pH 8.0, or 0.05 M Mops, pH 7.2. In the case of the spectrophotometric assay, samples additionally contained 30 units/mL glutamic acid dehydrogenase, 0.25 mM NADH/H^+, and 15 mM α-ketoglutaric acid. Reactions were started by addition of QC, and activity was monitored by recording the decrease in absorbance at 340 nm. In contrast, the assay samples for fluorometric detection of QC activity contained only buffer and 0.4 unit/mL pyroglutamyl aminopeptidase as the auxiliary enzyme. The excitation/emission wavelengths were 380/460 nm (H-Gln-AMC) or 320/410 nm (H-Gln-βNA). Reactions were started by addition of QC. QC activity was determined from a standard curve of the fluorophore under assay conditions. All determinations were carried out at 30 °C using the BMG Novostar reader for microplates.

For inhibitor testing, the sample composition was the same as described above, except for the added putative inhibitory compound. Inhibitory constants were determined using H-Gln-AMC in a concentration range between 0.25 and 4 K_M. The fluorometric assay using H-Gln-βNA was applied to investigate the pH dependence of the catalytic specificity. In these studies the reaction buffer consisted of 0.025 M acetic acid, 0.025 M Mes, and 0.05 M Tris-HCl, adjusted to the desired pH using HCl or NaOH. The buffer assures a constant ionic strength over a very broad pH range (*24*). Evaluation of the acquired enzyme kinetic data was performed using the equation:

$$k_{cat}/K_M(\mathrm{pH}) = k_{cat}/K_M(\mathrm{limit})[1/(1 + [H^+]/K_{HS} + K_{E1}/[H^+] + K_{E1}/[H^+]K_{E2}/[H^+])]$$

in which k_{cat}/K_M(pH) denotes the pH-dependent (observed) kinetic parameter. k_{cat}/K_M(limit) denotes the pH-independent ("limiting") value. K_{HS}, K_{E1}, and K_{E2} denote the dissociation constants of the substrate amino group and two dissociating groups of the enzyme, respectively. Evaluation of all kinetic data was performed using GraFit software (version 5.0.4 for windows; Erithacus Software Ltd., Horley, U.K.).

Preparation of ApoDromeQC. DromeQC (4.0 mL, 7 mg/mL) was inactivated by dialysis against 1.0 L of buffer containing 5.0 mM 1,10-phenanthroline, 5.0 mM EDTA, and 500 mM NaCl in 50.0 mM Hepes, pH 7.5. Inactivation was carried out for 8 h, including a buffer change after 4 h. The chelating agents were separated from the apoenzyme by dialysis against 1.0 L of 10 mM Hepes, pH 7.5, containing 50 g of Chelex-100 (Bio-Rad, Munich, Germany). The buffer was changed two times, after 6 and 12 h of dialysis. The final dialysis was performed overnight. All buffers were prepared in metal-free polystyrene containers. Subsequently, the apoenzyme was centrifugated at 20000*g* for 1 h at 4 °C, and the protein concentration was determined at 280 nm (*25*). Reactivation experiments were carried out by adding 20 μL of transition metal solution, prepared in water (UltraPure; Merck, Darmstadt, Germany), to 20 μL of apoenzyme at room temperature for 15 min. Finally, enzymatic activity was assessed as described above, except that 1 mM EDTA was added to the reaction buffer in order to avoid rapid reactivation of the enzyme by adventitious zinc ions present in the buffers.

TXRF and CD Spectroscopic Evaluations. DromeQC was desalted by size-exclusion chromatography using a Sephadex G-25 fast desalting column (1.0 × 10 cm), which was preequilibrated in 10 mM Tris-HCl, pH 7.6. Afterward, the protein was concentrated to 3−4 mg/mL by ultrafiltration and the metal content analyzed. The elution buffer was used as a background control. Element analysis was performed using TXRF essentially as described elsewhere (*22*). Five microliters of undiluted sample solution or control buffer was applied onto the TXRF quartz glass sample support and

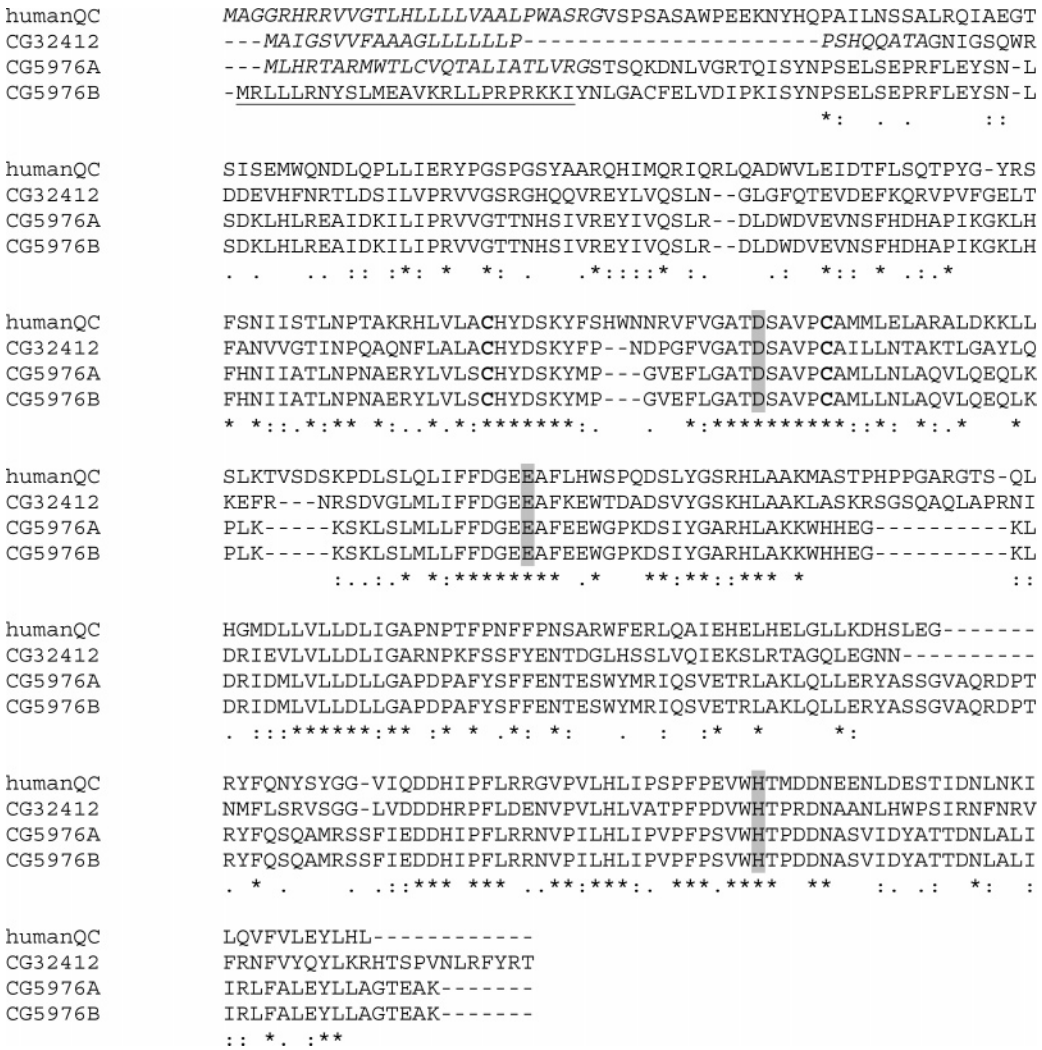

FIGURE 1: Sequence alignment of human QC and putative homologous proteins from *Drosophila melanogaster*. Multiple sequence alignment was performed using ClustalW at ch.EMBnet.org with default settings. The conservation of the complexing residues of the active site is indicated by the gray boxes. Two cysteine residues, which are located close to the active site in human QC and which form a disulfide bond, are also conserved and depicted in bold. Secretion signals are highlighted in italics, and the mitochondrial targeting peptide of CG5976, isoform B, is underlined. The proteins deduced from genes CG5976 and CG32412 display approximately 41% and 38% sequence identity with human QC, respectively.

dried under IR radiation. Afterward, 5 μL of diluted Se aqueous standard solution (internal standard; Aldrich) was added to each sample and dried again. The signals of X-ray fluorescence were allowed to be collected in 100 s. Three replicates were prepared. For all determinations, an Extra II TXRF module containing molybdenum and tungsten primary X-ray sources (Seifert, Ahrensburg, Germany) connected to a Link QX 2000 detector/analyzed device (Oxford Instruments, New Wycombe, U.K.) was used. The X-ray sources were operated at 50 kV and 38 mA.

CD spectra of *Drosophila* QCs in 10.0 mM phosphate buffer, pH 6.8, were acquired with a Jasco J-715 spectrapolarimeter using quartz cuvettes of 0.1 cm path length. The mean of 10 scans between 190 and 260 nm was calculated and corrected by subtraction of the buffer spectra. The percentage of secondary structure elements was calculated using the Jasco secondary structure estimation program based on the method of Yang (*26*).

RESULTS

Identification of Putative Drosophila QCs. On the basis of the coding region of human QC, database mining identified genes encoding homologous proteins from *D. melanogaster*. A first run revealed the gene products of CG32412, CG5976, and CG6168, all located on chromosome 3L as putative QCs. Analysis uncovered, however, that CG6168 was not organized in an exon/intron structure and no mRNA was described before, strongly implying a pseudogene. In contrast, database mining identified transcripts of genes CG32412 and CG5976. Surprisingly, the structure of CG5976 supports formation of two proteins, which are formed from different mRNAs. The resulting proteins differ only in their N-terminal region (Figure 1). The overall sequence identity of CG32412 and CG5976 with human QC is 38% and 41%, respectively. Interestingly, the putative QC proteins from *Drosophila* share only about 38% sequence identity, which might reflect functional differences. On the basis of CG5976, proteins of 354 or 352 amino acids could be deduced, which is similar to the length of human QC (361 aa). The second gene CG32412 encodes a truncated protein of 340 amino acids. All putative QC proteins contain two conserved cysteine residues, which have been identified to form a disulfide bond in human QC (*20*). Furthermore, the amino acids chelating the active site zinc ion, which is

responsible for activity and inhibitor binding (*10*, *17*, *27*), are also conserved in the homologous proteins from *Drosophila*. Appreciable differences in the primary structure were obvious for the N-termini of the proteins. In human QC, the N-terminus encodes a signal sequence for the cotranslational transport of the protein into the secretory pathway. Accordingly, signal sequences were also identified in CG32412 and isoform A of CG5976. Intriguingly, several different predictions provided evidence that the protein deduced from isoform B of CG5976 does not contain an N-terminal secretion signal. Instead, a high probability of 79% and 97% for an export to mitochondria was observed, computed using the programs TargetP and Mitoprot (*28*, *29*), respectively (available at www.expasy.ch). The latter is also supported by the clustering of positively charged residues at the N-terminus.

Homologous Expression in S2 Drosophila Cells. On the basis of the genes CG5976 and CG32412, cDNAs were ordered encoding the deduced proteins from nucleotide entries GH11174, RE53796, and RE61650. On the basis of the different predictions concerning the localization, the gene products were named isoDromeQC and DromeQC, repectively. In order to assess whether the isolated cDNAs encode active QCs, the open reading frames were cloned into a pMTV5HisB vector and expressed in Schneider (S2) cells. According to the predictions, which were based on the deduced primary structures, subcellular localization is mediated by the N-terminal sequence in either case. Therefore, also clones were generated, which express the proteins with a C-terminal poly-His or V5 epitope fusion, enabling also immunohistochemical analyses.

Expression of DromeQC and both isoDromeQC cDNAs resulted in detectable QC-like enzymatic activity (Figure 2A). Moreover, a subcellular fractionation experiment clearly proofs differences in the distribution of the QC proteins. According to the prediction, the highest DromeQC activity was identified in the medium of the cultured cells, implying secretion of the enzyme. In contrast, the medium of cells expressing isoDromeQC(B) was virtually free of QC activity. Instead, the highest activity was determined in the fraction containing the cell debris and in the heavy membrane fraction, which is enriched for mitochondria. Furthermore, the introduction of the C-terminal tag did not alter the activity distribution pattern significantly, substantiating that the subcellular localization is mediated by the N-terminus. The compartmentalization of the V5-tagged isoDromeQC(B) was verified by immunostaining (Figure 2B). Mitochondria of S2 cells were labeled using Mitotracker and fixed, and isoDromeQC was detected by an anti-V5 antibody. The double staining of the cells confirms the mitochondrial localization of the target protein and thus the result of the subcellular fractionation experiment.

Heterologous Expression and Purification of Drosophila QCs. In order to characterize the QC from *Drosophila* on the molecular level, both proteins were expressed heterologously and purified. In analogy to the subcellular distribution in *Drosophila* cells, secretory expression in the yeast *P. pastoris* was implemented for DromeQC. The native signal sequence was substituted for the α-leader pre-prosequence of yeast, in order to promote an efficient translocation into the secretory pathway of *Pichia*. Owing to the expression construct, the recombinant DromeQC is secreted into the

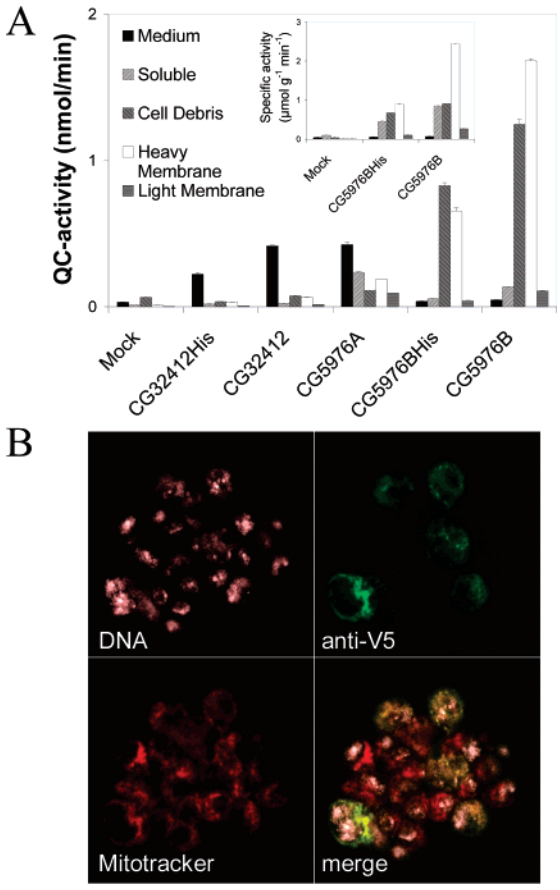

FIGURE 2: Analysis of the subcellular distribution of QC activity following expression of cDNAs deduced from genes CG5976 and CG32412 in Schneider (S2) cells. (A) Expressing cells were subjected to subcellular fractionation, and the QC activity was determined. The highest QC activity following expression of CG32412 and CG5976A cDNA was determined in the culture medium, implying secretion. In contrast, expression of CG5976B cDNA resulted in highest activities and specific activities (inset) in the cell debris and the heavy membrane fraction, suggesting mitochondrial localization. According to the prediction, cellular localization was apparently mediated by the N-terminus, since C-terminal His fusions did not alter the pattern significantly. (B) Immunochemical imaging of the subcellular localization of an isoDromeB-V5 fusion protein. Transiently transfected S2 cells were fixed and stained by applying Mitotracker (red) and DAPI. IsoDromeQC was immunologically labeled with a V5 epitope antibody followed by an Alexa-conjugated secondary antibody (green). The localization of isoDromeQC supports a mitochondrial localization of the protein.

medium of the expressing cells. Indeed, QC activity was detected in the medium of stably transfected yeast cells after induction of expression by methanol. Moreover, expression of DromeQC in a 5.0L bioreactor resulted in an exceptionally high yield of approximately 800 mg/L fermentation broth.

However, an attempt to express isoDromeQC in the secretory pathway of yeast failed. QC activity could not be detected in the medium of the recombinants following induction by methanol (data not shown). Instead, high amounts of isoDromeQC were obtained following expression of the mature protein in *E. coli*. The N-terminal signal sequences and the six following amino acids were replaced by a vector-encoded sequence containing a polyhistidine tag. The N-termini of the DromeQC and isoDromeQC constructs are illustrated in Figure 3. Since the isoDromeQC forms A and B differ only at their N-terminus (Figure 1), the

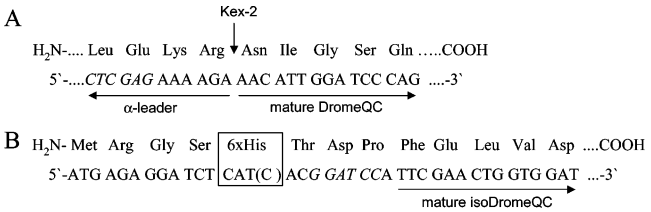

FIGURE 3: Schematic illustration of the N-terminal regions of DromeQC and isoDromeQC, which are generated in heterologous expression in *P. pastoris* and *E. coli*, respectively. Due to the restriction of the differences between CG5976 A and B to the N-terminus (Figure 1), the expressed isoDromeQC virtually resembles both proteins.

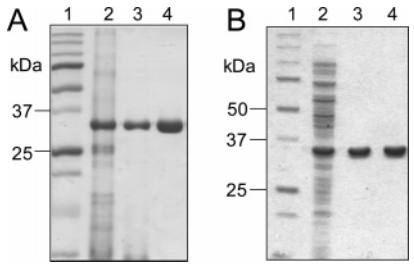

FIGURE 4: Characterization of DromeQC and isoDromeQC using SDS−PAGE. (A) SDS−PAGE illustrating the purification procedure of DromeQC. Lanes: 1, molecular mass standards (kDa); 2, fermentation medium after expression; 3, DromeQC-containing fraction after cation-exchange chromatography; 4, purified DromeQC after hydrophobic interaction chromatography. (B) SDS−PAGE illustrating the purification procedure of isoDromeQC. Lanes: 1, molecular mass standards (kDa); 2, supernatant after high-pressure homogenization and centrifugation; 3, isoDromeQC-containing fraction after IMAC; 4, purified DromeQC after hydrophobic interaction chromatography.

recombinantly expressed protein resembles both forms very well.

The purification of DromeQC and isoDromeQC is illustrated in Figure 4. The procedures were initiated by expanded bed adsorption on a cation-exchange resin or a chelating material. Both proteins were further purified by hydrophobic interaction chromatography. Due to the exceptionally high expression rates in the heterologous systems, homogeneous protein was obtained after two chromatographic steps. A typical purification procedure of DromeQC and isoDromeQC is listed in Table 2. For analysis of the metal content, an untagged isoDromeQC was expressed in *E. coli* and purified by applying hydrophobic interaction chromatography, anion-exchange chromatography and size-exclusion chromatography (not shown).

Enzymatic Characterization. Due to the relatively low sequence identity between DromeQC and isoDromeQC, it is tempting to suspect differences in the substrate specificity of both enzymes. For detailed analysis, a set of different substrates was investigated (Table 3). Interestingly, the observed specificities are very similar for both QCs at a first glance. Both enzymes converted all applied substrates with very similar k_{cat}/K_M values. As also observed previously for human and murine QC, conversion of dipeptides was less efficient compared to the dipeptide surrogates and the tri- and tetrapeptides. The relative preference for substrates containing hydrophobic amino acids suggests also primarily hydrophobic secondary interactions in the active site. Striking is the low specificity for negatively charged substrates, e.g., Gln-Glu and Gln-Asp-Glu-Leu, in comparison to uncharged

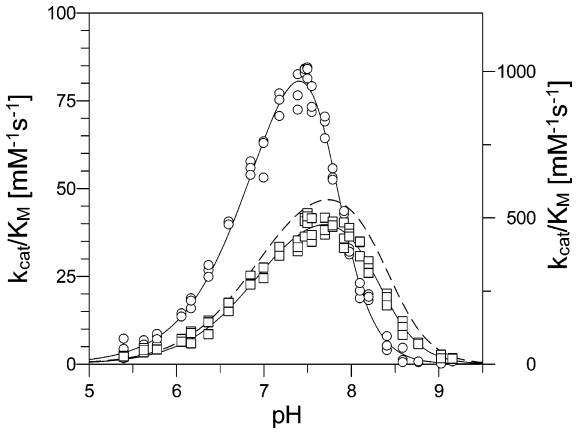

FIGURE 5: pH dependence of DromeQC (circles) and isoDromeQC (squares) determined under first-order rate conditions using Gln-βNA as substrate. In all cases, a buffer system providing a constant ionic strength according to Ellis and Morrison (*24*) was applied, consisting of 25 mM MES, 25 mM acetic acid, and 50 mM Tris-HCl. The rate profiles were evaluated by fitting the data according to equations that account for three two dissociating groups, assuming that the protonated substrate is not converted. The dotted trace represents the pH dependence of murine QC.

Table 2: Purification Scheme of Recombinant DromeQC and IsoDromeQC Following Expression in *P. pastoris* and *E. coli*, Respectively

	purification step	protein (mg)	QC activity (units)	specific activity (units/mg)	yield (%)
DromeQC	medium	2180	3010	1.4	100
	IEX	291	716	2.5	24
	HIC	121	420	3.5	14
isoDromeQC	homogenate	10800	7635	0.7	100
	IMAC	2046	5278	2.6	68
	HIC	1704	4897	2.9	67

or positively charged di- and tetrapeptides. Such a suspicious repulsion of negative substrates was not observed in previous studies with human and murine QC (*21*, *22*). The effect of the charged residues was partially compensated by adjacent hydrophobic amino acids, as evidenced by the relatively high specificity for Gln-Glu-Tyr-Phe.

The substrate specificity constants (k_{cat}/K_M) of both *Drosophila* QCs were found about 1 or 2 orders of magnitude lower in comparison to mammalian QCs. The differences depended mainly on higher K_M values, suggesting differences in the substrate binding modes (not shown).

In order to further characterize the specificity of the enzymes, the pH dependence of catalysis was assessed. Interestingly, DromeQC displayed a very narrow pH optimum at pH 7.0−7.5. In contrast, the optimal pH for isoDromeQC was between pH 7.5−8, thus more similar to the mammalian enzymes (Figure 6). The kinetic data were evaluated by applying a model, which considers three dissociating groups: one of the substrate and two of the enzyme. The pK_a of the applied substrate Gln-βNA was determined previously to be 6.97 ± 0.01 (*8*). Assuming that the deprotonated substrate is only converted, one part of the bell-shaped curve in the pH region between pH 5 and pH 7 was explained. The nonsymmetric character of the bell-shaped curve was evaluated assuming two groups, which confer enzymatically inactivation upon deprotonation. Fitting of these data resulted in pK_a values of 9.1 ± 0.4 and 6.4 ± 0.3 for DromeQC and 8.7 ± 0.1 and 7.9 ± 0.2 for

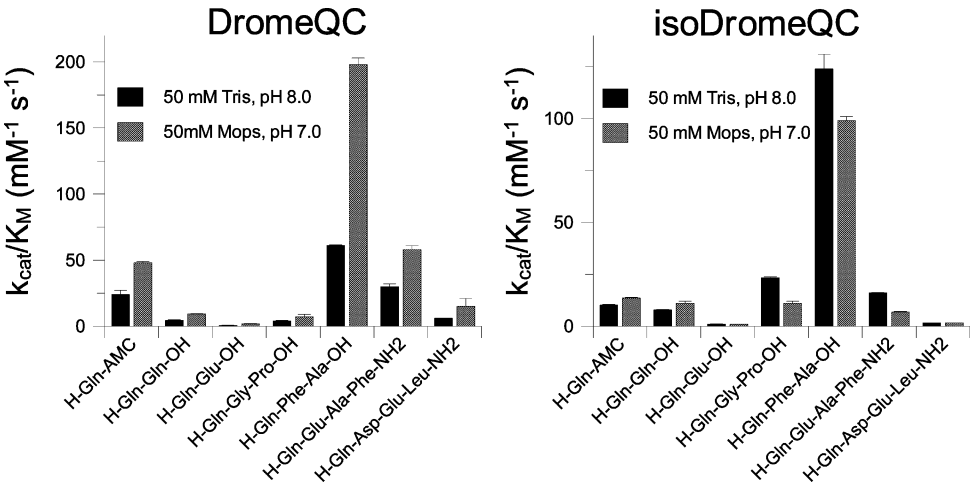

FIGURE 6: Catalytic specificities of recombinant DromeQC and isoDromeQC at pH 7.0 and 8.0. The differences in the pH dependence of catalysis for Gln-βNA (Figure 5) are reflected by the specificities for other substrates as well. The different specificities at the two pH values were caused by changing K_M values, suggesting an influence of pH on substrate binding. The conversion of peptide substrates was monitored using glutamic dehydrogenase as the auxiliary enzyme, and cyclization of Gln-AMC was analyzed by applying pyroglutamyl aminopeptidase. All reactions were carried out at 30 °C.

Table 3: Catalytic Parameters of QC-Catalyzed pGlu Formation of Substrates of Varying Length and Charge[a]

	DromeQC			isoDromeQC			murine QC
substrate	K_M (mM)	k_{cat} (s^{-1})	k_{cat}/K_M (mM^{-1} s^{-1})	K_M (mM)	k_{cat} (s^{-1})	k_{cat}/K_M (mM^{-1} s^{-1})	k_{cat}/K_M (mM^{-1} s^{-1})
H-Gln-AMC	0.31 ± 0.04	7 ± 2	24 ± 3	0.205 ± 0.008	2.09 ± 0.03	10.2 ± 0.3	98 ± 2
H-Gln-βNA[b]	0.17 ± 0.01	1.3 ± 0.3	7.4 ± 1.1	0.15 ± 0.01	1.1 ± 0.1	7.4 ± 0.3	294 ± 6
H-Gln-Gly-OH	7.1 ± 0.2	9 ± 3	1.3 ± 0.4	2.4 ± 0.5	4.9 ± 0.6	2.1 ± 0.2	53 ± 1
H-Gln-Ala-OH	5.0 ± 0.3	17 ± 1	3.48 ± 0.06	2.8 ± 0.1	16 ± 4	6 ± 1	247 ± 4
H-Gln-Gln-OH	1.5 ± 0.2	7 ± 1	4.5 ± 0.3	0.94 ± 0.05	7.4 ± 0.5	7.9 ± 0.2	140 ± 2
H-Gln-Glu-OH	29.5 ± 7.4	38 ± 17	1.3 ± 0.3			0.85 ± 0.09	58 ± 1
H-Gln-Gly-Pro-OH	4.1 ± 0.4	16 ± 3	3.9 ± 0.5	1.17 ± 0.06	14 ± 2	23.4 ± 0.4	195 ± 7
H-Gln-Tyr-Ala-OH				0.72 ± 0.02	17.04 ± 0.03	0.72 ± 0.02	930 ± 27
H-Gln-Phe-Ala-OH	0.35 ± 0.04	22 ± 2	61.2 ± 0.3	0.128 ± 0.003	16 ± 1	124 ± 7	1812 ± 64
H-Gln-Val-Ala-OH	0.14 ± 0.01	5.3 ± 0.4	38.7 ± 0.2	0.1293 ± 0.0005	3.02 ± 0.07	23.4 ± 0.4	
H-Gln-Glu-Tyr-Phe-NH_2	0.065 ± 0.004	6.9 ± 0.5	106 ± 1				979 ± 62
H-Gln-Glu-Ala-Phe-NH_2	0.42 ± 0.03	12.7 ± 0.2	30 ± 2	0.68 ± 0.04	11.0 ± 0.8	16.2 ± 0.1	1000 ± 51
H-Gln-Asp-Glu-Leu-NH_2	2.3 ± 0.2	14 ± 1	5.9 ± 0.2			1.7	833 ± 21
H-Gln-Lys-Arg-Leu-NH_2	0.08 ± 0.02	7.0 ± 0.1	90 ± 17				619 ± 25

[a] Reactions were carried out at 30 °C. [b] Substrate inhibition detected.

isoDromeQC. Thus, the apparently only one dissociating group influencing the catalytic specificity is different between both enzymes.

The different pH dependencies were also observed for other substrates (Figure 6). DromeQC displayed an increased specificity at pH 7 for all analyzed substrates. The specificity of isoDromeQC remained virtually unchanged. The results substantiate the hypothesis that the drop in specificity at basic pH is due to dissociating groups of the enzyme. The increase in DromeQC specificity at pH 7 was due to decreasing K_M values; k_{cat} remained virtually unchanged in every case (not shown). Therefore, the observed changes in specificity can be attributed to differences in substrate binding.

In previous studies, it has been shown that the mammalian QCs are competitively inhibited by imidazole and cysteamine derivatives (*17*, *22*). Therefore, several different compounds of both inhibitory classes were analyzed in terms of their inhibitory potency toward DromeQC and isoDromeQC activity (Table 4). As observed analyzing the substrate specificity, differences were also found for inhibitor binding between mammalian and *Drosophila* QC. All compounds tested inhibited the *Drosophila* QCs linear competitively (not shown), as was observed for human and murine QC. The inhibitory potency, however, was reduced compared to the mammalian enzymes.

Intriguingly, the binding of the imidazoles also reflects the different pH dependencies of catalysis. While the K_i values remained virtually unchanged between pH 7 and pH 8 with isoDromeQC, the K_i values dropped in the case of DromeQC at pH 7. This suggests a relation of the observed pH dependencies of inhibition and substrate specificity. In contrast, the K_i values of the cysteamine derivatives were increased at pH 7, implying different binding modes of this inhibitor class. This phenomenon was already previously investigated using murine QC (*22*).

Summarizing, also with respect to inhibitor binding, isoDromeQC appears to be more similar to the mammalian QCs, as finally evidenced by the pH dependence and inhibitory potency of P150/03, a highly potent inhibitor of human and murine QC.

Spectroscopic Characterization of Drosophila QCs. The inhibitory specificity of the QCs from *Drosophila* and the conservation of the zinc-chelating residues between invertebrate and mammalian QCs (Figure 1) implied similar

Table 4: Inhibition Constants of Competitive Inhibitors[a]

	DromeQC		isoDromeQC		murine QC
inhibitor	K_i (pH 8) (μM)	K_i (pH 7) (μM)	K_i (pH 8) (μM)	K_i (pH 7) (μM)	K_i (pH 8) (μM)
imidazoles					
imidazole	1141 ± 36	304 ± 19	364 ± 2	405 ± 11	160 ± 10
benzimidazole	2188 ± 128	549 ± 81	1447 ± 221	671 ± 38	192 ± 3
1-benzylimidazole	48 ± 5	13 ± 1	19 ± 1	17 ± 1	6.4 ± 0.7
1-methylimidazole	109 ± 7	36 ± 1	103 ± 15	114 ± 6	23 ± 1
P150/03	3.14 ± 0.05	0.94 ± 0.09	0.097 ± 0.005	0.101 ± 0.002	
N-ω-acetylhistamine	84 ± 5	39.1 ± 0.5	140 ± 4	145 ± 2	
4-methylimidazole	73 ± 3				
cysteamines					
cysteamine	56 ± 9	301 ± 10	205 ± 14	827 ± 23	42 ± 1
N-dimethylcysteamine	79 ± 8	80 ± 4	63 ± 7	154 ± 1	29 ± 2
N-diethylcysteamine	93 ± 5				10.9 ± 0.3

[a] Due to the different pH dependence of catalysis, K_i values were determined at pH 7 and 8. Reactions were carried out at 30 °C, and Gln-AMC was applied as the assay substrate.

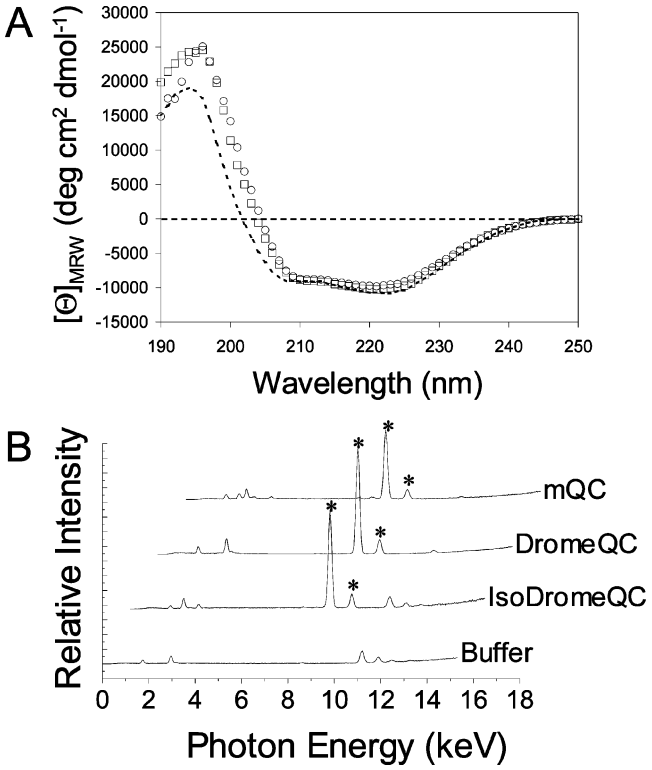

FIGURE 7: Spectroscopic characterization of Drome and isoDromeQC. (A) CD spectroscopic structure analysis of DromeQC (circles) and isoDromeQC (squares). For comparison, the CD spectrum of murine QC is depicted as a dotted trace. The protein was dissolved in 10 mM potassium phosphate buffer, pH 6.8. (B) Superposition of total reflection X-ray fluorescence (TXRF) spectra of DromeQC, isoDromeQC, and murine QC (mQC). Protein concentrations were 110, 93, and 81 μM, respectively. Prior to analysis, the proteins were desalted by size-exclusion chromatography using 10 mM Tris-HCl, pH 7.6, as the running buffer. An asterisk assigns signals corresponding to zinc. The evaluation of the measurements revealed equimolar zinc content in all animal QCs.

structural features of the enzymes and a similar metal-dependent mode of catalysis. In order to prove also *Drosophila* QCs as metalloenzymes, the mature recombinant proteins were concentrated to an approximately 100 μM concentration, desalted, and subjected to total X-ray fluorescence spectroscopic analysis (TXRF) to determine the specific metal content of the enzyme (Figure 7B). As previously observed with mammalian QCs, prominent zinc signals were obtained in DromeQC and isoDromeQC preparations. A quantification of the zinc signals revealed relative zinc contents of 0.93 and 0.87 mol of zinc/mol of DromeQC or isoDromeQC, respectively. In conclusion, also the invertebrate QCs were identified as single-zinc metalloenzymes.

The structural homology of the *Drosophila* QCs is further reflected by a CD spectroscopic analysis (Figure 7A). Both QCs generate virtually identical far-UV spectra, indicating an identical fold of the peptide chain. Furthermore, the prominent minimum at 220 nm and the depleted ellipticity at 200 nm imply a dominating α-helical content in the proteins. The analysis of the crystal structure of human QC displayed about 40% α-helix and 19% β-sheet. Thus, the invertebrate QCs seem to share an identical fold to the mammalian counterparts.

DISCUSSION

Several mammalian hormones, e.g., thyrotropin-releasing hormone, gonadotropin-releasing hormone, and gastrin, contain an N-terminal pGlu residue. Presumably, the major function of the pGlu residue is to provide stability against degradation by aminopeptidases, thus prolonging the physiological half-life of these peptides (*30*). For several hormones, a crucial role of the N-terminus for binding to the respective receptor is described (*31*). In mammals, the formation of pGlu hormones and proteins is catalyzed by the enzyme glutaminyl cyclase. The presence of pyroglutamyl peptides, preferably neuropeptides, has been also described in arthropods and even in the mollusk *Aplysia*, strongly implying evolutionary conserved mechanisms of pGlu peptide functions and their formation (*15*, *32*, *33*). The isolation of glutaminyl cyclases from *D. melanogaster* described here strongly implies evolutionarily well-conserved mechanisms of pGlu peptide formation and, presumably, represents an effective machinery to confer hormonal activity.

The analysis of the enzymatic properties of the *Drosophila* QCs evidences also a well-conserved enzyme class between invertebrates and vertebrates. In spite of the moderate sequence identity between the DromeQCs and their mammalian counterparts, the general catalytic properties appear to be well conserved. All animal QCs have been identified as single-zinc metalloenzymes, with an essential role of the metal ion for catalysis. The mechanism of substrate recogni-

Secretory Pathway

Corazonin	*MLRLLLLPLFLFTLSMCMG*	QT...
Adipokinetic hormone	*MNPKSEVLIAAVLFMLLACVQC*	QL...
Attacin-C	*MSKIVLLIVVIVGVLGSLAVALP*	QR...

Mitochondrial Precursors

Acyl-CoA Dehydrogenase	*MAFLNKLAAPALRQLVS*	QS...
Succinate Dehydrogenase	*MSGIMRVPSILAKNAVASMQRAAAVGVQRSYHITHGRQ*	QA...
Propionyl-CoA Dehydrogenase	*MIRLNWLFRSSSVLLRS*	QV...

FIGURE 8: N-Terminal protein sequences of putative QC substrates in *Drosophila*. The secretory proteins are cotranslationally translocated into the ER, mediated by the N-terminal signal peptide. After cleavage by the signal peptidase, a glutaminyl or glutamyl residue is demasked that is prone to cyclization catalyzed by DromeQC or isoDromeQC-A. Similarly, the putative mitochondrial proteins display an N-terminal transit peptide sequence, which mediates transport into the lumen of mitochondria. Protein sequences were obtained from the SwissProt database (www.expasy.ch), and mitochondrial transit peptide cleavage sites were predicted using Mitoprot (*28*, *29*).

tion, i.e., the preference for hydrophobic amino acids adjacent to the N-terminal glutamine residue, the repulsion of negatively charged substrates, and the requirement of an unprotonated substrate amino group have been observed with the mammalian and the *Drosophila* QCs, suggesting similar conditions in the active sites.

Completely novel is, however, the identification and isolation of isoforms of QC in *Drosophila*. Interestingly, both *Drosophila* QCs differ from the mammalian enzymes to a similar extent (Figure 1), which does actually not reveal a clear evolutionary relationship of the mammalian QCs and one of the counterparts from *Drosophila*. The enzymatic analysis, however, revealed subtle differences between the DromeQCs. At first, the pH dependence of the enzymatic specificity differs between DromeQC and isoDromeQC. While DromeQC shows a very narrow pH dependence with an optimum near pH 7.0, isoDromeQC resembles the pH characteristic of the mammalian QCs, displaying an optimum at mildly basic pH. The differences could be explained by a different pK_a of one of the enzymic groups influencing the specificity constant k_{cat}/K_M, thus suggesting differences in the micromilleu of the active sites. A second hint, which tempts us to speculate that isoDromeQC is evolutionary more related to the mammalian QCs, is provided by the pH dependence of the inhibitory specificity. While the potency of imidazole-derived inhibitors was increased at pH 7.0 with DromeQC, virtually unchanged K_i values were observed with isoDromeQC, which is in correspondence to the mammalian enzymes. Finally, a potent inhibitor of human QC, P150/03 (K_i = 60 nM), displayed a similar potency against isoDromeQC but a drop of potency of 1−2 orders of magnitude interacting with DromeQC, suggesting differences in the secondary interaction modes of the inhibitor and both QC isoforms.

The drastically decreasing specificity constants at basic pH were observed with all animal QCs investigated thus far. Intriguingly, the pH dependence characteristics of murine QC, DromeQC, and isoDromeQC support one common pK_a in this region of 8.9, 9.1, and 8.7, respectively [Figure 5 (*22*)]. Furthermore, in murine QC this dissociating group influences imidazole inhibition as well. From the additional data obtained using the homologous QCs from *Drosophila*, we suggest that these pK_a are due to deprotonation of the zinc-bound water molecule. In the resting state, the zinc ion is coordinated to a single histidine, aspartic acid, and glutamic acid as ligands. The fourth coordination site is conjugated to a water molecule, which can be displaced by the substrate or the imidazole-based inhibitor. Upon deprotonation of this water molecule at basic pH, the resulting hydroxyl ion displacement by weak ligands fails; hence, the specificity drops. In contrast, the deprotonated thiol group of cysteamine derivatives still enables efficient activity at basic pH due to the increased nucleophilicity and may substitute the hydroxyl ion at the Zn-coordination site (Table 4). A clarification of this suggestion might be provided by the crystal structure of an animal QC in conjunction with a cysteamine-derived inhibitor.

The differences in the catalytic specificity of DromeQC and isoDromeQC make sense in light of their subcellular distribution: Due to the distribution of DromeQC in the acidic environment of the secretory pathway, the higher specific activity at acidic pH compared to isoDromeQC and the lower pH optimum appear conceivable. In contrast, conversion of the substrates of isoDromeQC in mitochondrial lumen takes place at neutral to mildly basic pH, thus in the optimal pH region for isoDromeQC. The secretion signal at the N-terminus makes DromeQC and isoDromeQC(A) to be likely catalysts of pGlu hormone maturation in *Drosophila*. As described previously for the mammalian QCs, proteolytic demasking of an N-terminal glutaminyl residue in the ER or Golgi must precede the pyroglutamyl formation (Figure 8). However, physiological substrates of isoDromeQC(B) are still unknown. A first database mining uncovered two human mitochondrial proteins putatively containing an N-terminal pGlu residue, aconitase, and the α chain of ATP synthase. Similar to the processing of the substrates in the secretory pathway, a N-terminal glutaminyl residue is proteolytically generated by cleavage of the mitochondrial transit peptide, which is followed by cyclization. The role of the pGlu modification in the mitochondrial proteins is completely unknown and will be the subject of further investigations; however, the data might raise the possibility that it is conserved in arthropods and mammals.

Concluding, the isolation and characterization of the QCs from *Drosophila* provide evidence that (a) the pGlu peptide formation in the animal kingdom is generally catalyzed by metalloenzymes, which is in contrast to the pGlu formation in plants (*34*), and (b) isoforms of glutaminyl cyclase are formed, at least in arthropods, which was proven for the first time. Finally, the subcellular distribution of QC activity to mitochondria supports yet undiscovered functions of the pGlu modifications in this cellular compartment. Deeper insights into the role of the glutaminyl cyclase in mitochondria can be obtained by isolation and characterization of *Drosophila* knockout flies of the genes CG5976 and CG32412.

ACKNOWLEDGMENT

We greatly appreciate the gift of P150/03 from Dr. Ulrich Heiser, (Medicinal Chemistry Department, Probiodrug AG). Thanks are also due to Holger Cynis, Nadine Jänckel, Henning Breyhan, and Katrin Schulz for valuable technical assistance.

REFERENCES

1. Abraham, G. N., and Podell, D. N. (1981) Pyroglutamic acid. Non-metabolic formation, function in proteins and peptides, and

characteristics of the enzymes effecting its removal, *Mol. Cell. Biochem. 38*, 181−190.
2. Fischer, W. H., and Spiess, J. (1987) Identification of a mammalian glutaminyl cyclase converting glutaminyl into pyroglutamyl peptides, *Proc. Natl. Acad. Sci. U.S.A. 84*, 3628−3632.
3. Saido, T. C., Iwatsubo, T., Mann, D. M., Shimada, H., Ihara, Y., and Kawashima, S. (1995) Dominant and differential deposition of distinct beta-amyloid peptide species, A beta N3(pE), in senile plaques, *Neuron 14*, 457−466.
4. Ghiso, J., Revesz, T., Holton, J., Rostagno, A., Lashley, T., Houlden, H., Gibb, G., Anderton, B., Bek, T., Bojsen-Moller, M., Wood, N., Vidal, R., Braendgaard, H., Plant, G., and Frangione, B. (2001) Chromosome 13 dementia syndromes as models of neurodegeneration. Amyloid, *Amyloid 8*, 277−284.
5. Cynis, H., Schilling, S., Bodnar, M., Hoffmann, T., Heiser, U., Saido, T. C., and Demuth, H. U. (2006) Inhibition of glutaminyl cyclase alters pyroglutamate formation in mammalian cells, *Biochim. Biophys. Acta 1764*, 1618−1625.
6. Busby, W. H. J., Quackenbush, G. E., Humm, J., Youngblood, W. W., and Kizer, J. S. (1987) An enzyme(s) that converts glutaminyl-peptides into pyroglutamyl-peptides. Presence in pituitary, brain, adrenal medulla, and lymphocytes, *J. Biol. Chem. 262*, 8532−8536.
7. Messer, M. (1963) Enzymatic cyclization of L-glutamine and L-glutaminyl peptides, *Nature 4874*, 1299.
8. Schilling, S., Hoffmann, T., Manhart, S., Hoffmann, M., and Demuth, H. U. (2004) Glutaminyl cyclases unfold glutamyl cyclase activity under mild acid conditions, *FEBS Lett. 563*, 191−196.
9. Wintjens, R., Belrhali, H., Clantin, B., Azarkan, M., Bompard, C., Baeyens-Volant, D., Looze, Y., and Villeret, V. (2006) Crystal structure of papaya glutaminyl cyclase, an archetype for plant and bacterial glutaminyl cyclases, *J. Mol. Biol. 357*, 457−470.
10. Huang, K. F., Liu, Y. L., Cheng, W. J., Ko, T. P., and Wang, A. H. (2005) Crystal structures of human glutaminyl cyclase, an enzyme responsible for protein N-terminal pyroglutamate formation, *Proc. Natl. Acad. Sci. U.S.A. 102*, 13117−13122.
11. Dahl, S. W., Slaughter, C., Lauritzen, C., Bateman, R. C., Jr., Connerton, I., and Pedersen, J. (2000) Carica papaya glutamine cyclotransferase belongs to a novel plant enzyme subfamily: cloning and characterization of the recombinant enzyme, *Protein Expression Purif. 20*, 27−36.
12. Pohl, T., Zimmer, M., Mugele, K., and Spiess, J. (1991) Primary structure and functional expression of a glutaminyl cyclase, *Proc. Natl. Acad. Sci. U.S.A. 88*, 10059−10063.
13. Sykes, P. A., Watson, S. J., Temple, J. S., and Bateman, R. C. J. (1999) Evidence for tissue-specific forms of glutaminyl cyclase, *FEBS Lett. 455*, 159−161.
14. Bockers, T. M., Kreutz, M. R., and Pohl, T. (1995) Glutaminyl-cyclase expression in the bovine/porcine hypothalamus and pituitary, *J. Neuroendocrinol. 7*, 445−453.
15. Baggerman, G., Cerstiaens, A., De Loof, A., and Schoofs, L. (2002) Peptidomics of the larval *Drosophila melanogaster* central nervous system, *J. Biol. Chem. 277*, 40368−40374.
16. Schaffer, M. H., Noyes, B. E., Slaughter, C. A., Thorne, G. C., and Gaskell, S. J. (1990) The fruitfly *Drosophila melanogaster* contains a novel charged adipokinetic-hormone-family peptide, *Biochem. J. 269*, 315−320.
17. Schilling, S., Niestroj, A. J., Rahfeld, J.-U., Hoffmann, T., Wermann, M., Zunkel, K., Wasternack, C., and Demuth, H.-U. (2003) Identification of human glutaminyl cyclase as a metalloenzyme: Inhibition by imidazole derivatives and heterocyclic chelators, *J. Biol. Chem. 278*, 49773−49779.
18. Crosby, M. A., Goodman, J. L., Strelets, V. B., Zhang, P., and Gelbart, W. M. (2007) FlyBase: genomes by the dozen, *Nucleic Acids Res. 35*, D486−D491.
19. Igaki, T., Kanuka, H., Inohara, N., Sawamoto, K., Nunez, G., Okano, H., and Miura, M. (2000) Drob-1, a *Drosophila* member of the Bcl-2/CED-9 family that promotes cell death, *Proc. Natl. Acad. Sci. U.S.A. 97*, 662−667.
20. Schilling, S., Hoffmann, T., Rosche, F., Manhart, S., Wasternack, C., and Demuth, H. U. (2002) Heterologous expression and characterization of human glutaminyl cyclase: evidence for a disulfide bond with importance for catalytic activity, *Biochemistry 41*, 10849−10857.
21. Schilling, S., Manhart, S., Hoffmann, T., Ludwig, H.-H., Wasternack, C., and Demuth, H.-U. (2003) Substrate specificity of glutaminyl cyclases from plants and animals, *Biol. Chem. 384*, 1583−1592.
22. Schilling, S., Cynis, H., von Bohlen, A., Hoffmann, T., Wermann, M., Heiser, U., Buchholz, M., Zunkel, K., and Demuth, H. U. (2005) Isolation, catalytic properties, and competitive inhibitors of the zinc-dependent murine glutaminyl cyclase, *Biochemistry 44*, 13415−13424.
23. Schilling, S., Hoffmann, T., Wermann, M., Heiser, U., Wasternack, C., and Demuth, H.-U. (2002) Continuous spectrometric assays for glutaminyl cyclase activity, *Anal. Biochem. 303*, 49−56.
24. Ellis, K. J., and Morrison, J. F. (1982) Buffers of constant ionic strength for studying pH-dependent processes, *Methods Enzymol. 87*, 405−426.
25. Gill, S. C., and von Hippel, P. H. (1989) Calculation of protein extinction coefficients from amino acid sequence data, *Anal. Biochem. 182*, 319−326.
26. Yang, J. T., Wu, C. S., and Martinez, H. M. (1986) Calculation of protein conformation from circular dichroism, *Methods Enzymol. 130*, 208−269.
27. Buchholz, M., Heiser, U., Schilling, S., Niestroj, A. J., Zunkel, K., and Demuth, H. U. (2006) The first potent inhibitors for human glutaminyl cyclase: synthesis and structure-activity relationship, *J. Med. Chem. 49*, 664−677.
28. Bendtsen, J. D., Nielsen, H., von Heijne, G., and Brunak, S. (2004) Improved prediction of signal peptides: SignalP 3.0, *J. Mol. Biol. 340*, 783−795.
29. Claros, M. G., and Vincens, P. (1996) Computational method to predict mitochondrially imported proteins and their targeting sequences, *Eur. J. Biochem. 241*, 779−786.
30. Morty, R. E., Bulau, P., Pelle, R., Wilk, S., and Abe, K. (2006) Pyroglutamyl peptidase type I from *Trypanosoma brucei*: a new virulence factor from African trypanosomes that de-blocks regulatory peptides in the plasma of infected hosts, *Biochem. J. 394*, 635−645.
31. Goren, H. J., Bauce, L. G., and Vale, W. (1977) Forces and structural limitations of binding of thyrotrophin-releasing factor to the thyrotrophin-releasing receptor: the pyroglutamic acid moiety, *Mol. Pharmacol. 13*, 606−614.
32. Garden, R. W., Moroz, T. P., Gleeson, J. M., Floyd, P. D., Li, L., Rubakhin, S. S., and Sweedler, J. V. (1999) Formation of N-pyroglutamyl peptides from N-Glu and N-Gln precursors in *Aplysia* neurons, *J. Neurochem. 72*, 676−681.
33. Furukawa, Y., Nakamaru, K., Wakayama, H., Fujisawa, Y., Minakata, H., Ohta, S., Morishita, F., Matsushima, O., Li, L., Romanova, E., Sweedler, J. V., Park, J. H., Romero, A., Cropper, E. C., Dembrow, N. C., Jing, J., Weiss, K. R., and Vilim, F. S. (2001) The enterins: a novel family of neuropeptides isolated from the enteric nervous system and CNS of *Aplysia*, *J. Neurosci. 21*, 8247−8261.
34. Schilling, S., Stenzel, I., von Bohlen, A., Wermann, M., Schulz, K., Demuth, H. U., and Wasternack, C. (2007) Isolation and characterization of the glutaminyl cyclases from *Solanum tuberosum* and *Arabidopsis thaliana*: implications for physiological functions, *Biol. Chem. 388*, 145−153.

BI701043X